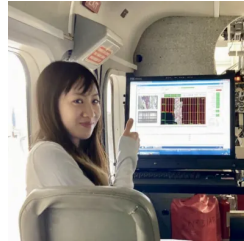


Does Tree Crown Architecture Differ by Tree Species? A test with NEON data

Yiting Fan¹, Ethan R. Cade¹, Conner W. Channels¹, G. Burch Fisher², Steven M. Guinn²,
Christopher Hughes¹, Lydia R. Nicolai¹, Andrew J. Elmore², Brenden E. McNeil¹

(1) Department of Geology and Geography, West Virginia University; (2) University of Maryland Center for Environmental Science, Appalachian Laboratory



PRESENTED AT:



1. BACKGROUND & HYPOTHESES

1.1. WHY CROWN ARCHITECTURE?

- Quantifying the health of forests is essential for predicting rates of climate change.
- Crown architecture strongly affects photosynthesis, evapotranspiration, and spectral reflectance that affect forest responses to climate change.
- It is the 3-D arrangement/orientation of leaves within a tree crown.

1.2. HYPOTHESES

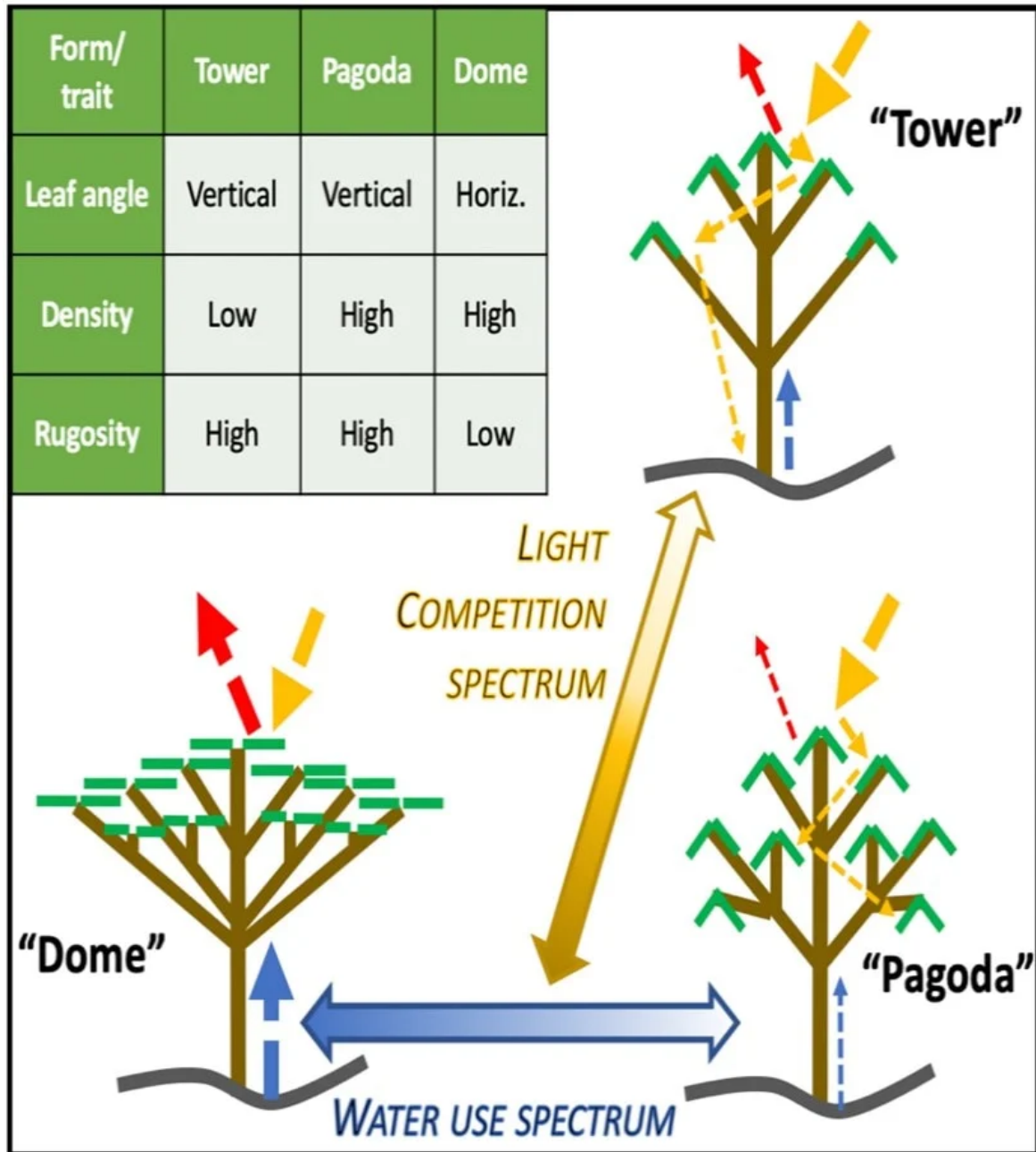


Fig 1: Hypothesized architectures (McNeil et al. 2023)

1.3. STUDY HIGHLIGHT

We quantify crown architectures and functioning of individual trees across diverse species and wide environmental gradients using NEON AOP airborne LiDAR & imaging spectroscopy, as well as NEON tower-based time-lapse photography.

2. OBJECTIVES & DATA OVERVIEW

We use measurements from 10 deciduous forest locations within the National Ecological Observatory Network (NEON) to quantify crown traits that can define key dimensions of variability in crown architecture across a wide environmental gradient.

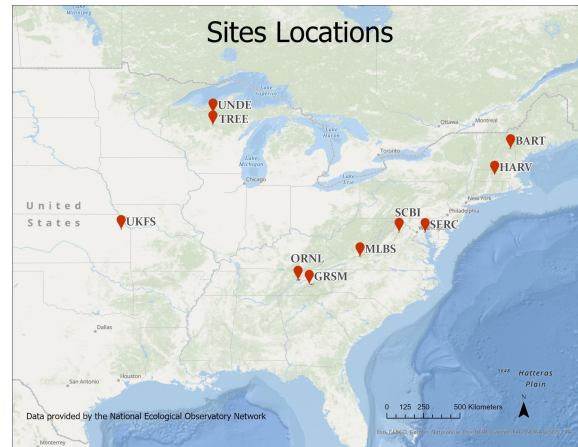


Fig 2: 10 NEON sites where we are processing NEON AOP LiDAR data and timelapse camera to measure tree crown architecture

Specifically, we: (1) quantify traits describing the density and distribution of leaves in tree crowns from NEON Airborne Observation Platform (AOP) LiDAR data; (2) measure seasonal trends in mean leaf angle (MLA) from tower-based time-lapse photography; (3) infer crown functioning from multi-scale data on several spectral indices as obtained from the NEON AOP imaging spectrometer and high-resolution camera.



Fig 3: Interior control (left) and underside view (right) of the NEON AOP DeHavilland DHC-6 Twin Otter aircraft that collects data 1000m above ground over NEON field sites during annual peak greenness. The payload consists of an imaging spectrometer, a discrete and waveform LiDAR instrument and a high-resolution digital camera



Fig 4: The automated time-lapse camera (upper) mounted to NEON flux tower at SCBI and SERC by two of our research undergrads (lower)

3. METHODS

3.1. AOP LIDAR

[VIDEO] https://res.cloudinary.com/amuze-interactive/video/upload/q_auto/v1701458053/agu23/39-8A-74-C4-8F-FA-BE-3C-D5-10-34-43-12-04-2D-19/Video/LITU_las_enhanced_online-video-cutter.com_vxtnb0.mp4

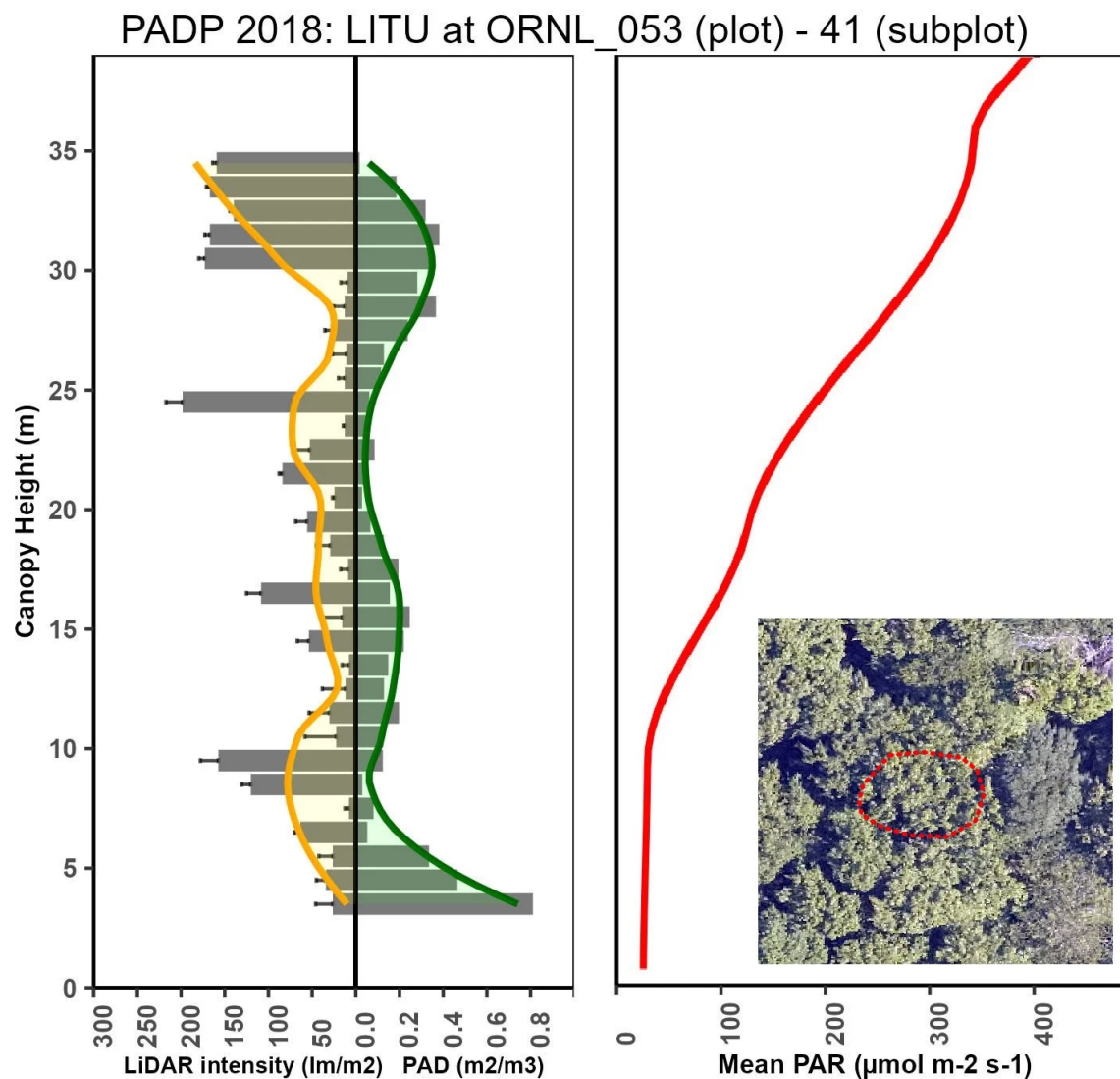


Fig 5: Example of AOP LiDAR point cloud (upper) within the delineated boundary (lower embedded photo) of a tuliptree at ORNL, TN, and its unfiltered vertical profiles of LiDAR intensity, plant area density (PAD) and PAR (lower)

- We quantify several traits for 197 crowns delineated by NEON terrestrial team, including plant/leaf area index (PAI/LAI), max canopy height (MAXCH), mean outer canopy height (MOCH), accumulative plant area density (APAD), accumulative LiDAR intensity (AInt), etc.
- We voxelize (1m) LiDAR point cloud and compute traits using established methods and open R packages, e.g., lidR (Roussel et al., 2020); leafR (de Almeida et al., 2019); canopyLazR (Kamoske et al., 2019).
- Data quality check:
 1. Invalid crowns are excluded by checking each delineation (Fig 5 lower embedded 0.1m-resolution photo).
 2. We use vertical profiles of photosynthetically active radiation (PAR) to cut off understorey noises by setting lower height threshold where tangent line of PAR starts to approach vertical (Fig 5 lower).

3. LiDAR intensity should attenuate by height (Fig 5).

3.2. MLA



Fig 6: Example of generating (x,y) leaf coordinates pairs for American beech at BART

- We use remote time-lapse cameras mounted level with sunlit treetops to take weekly leaf photos through growing season.
- From which we measure (x,y) coordinates pairs of petioles and tips of 75 leaves ((x,y) of 150 points).
- We compute species MLA from the (x,y) pairs.

3.3. SPECTRAL INDICES

We compute several spectral indices such as near-infrared reflectance of vegetation (NIRv) and their derived gray-level co-occurrence matrices for each crown.

3.4. SITE-SPECIES COMBO

From these data, we construct site-species trait combos and test for species difference and trait co-variations.

4. RESULTS & DISCUSSION

- Early successional tuliptrees (LITU, Fig 7) with a tower architecture (Fig 1) have more vertical leaves (Fig 8a) and higher rugosity (Fig 8b) than mid-successional black oak (QUVE) and red oak (QURU).
- Late-successional mesic sugar maple (ACSA) with a dome architecture has the most horizontal leaves (Fig 8a) and the lowest rugosity (Fig 8b), resulting in higher NIRv reflectance (Fig 9).
- We suggest that more vertical leaf angles allow lower leaves to receive more sunlight, an advantage for light harvesting in early-successional species to grow, but a disadvantage for shading out neighbors in late-successional species such as ACSA.
- Our APAD50 metric (Fig 8c & Fig 7) indicates that LITU has more "top-heavy" profile - leaves clustered at the top 50% of the crown, which fits with its production-oriented strategy focused on optimizing light harvesting at the expense of casting shade or conserving water. ACSA is more "bottom-heavy" with most leaves in the lower half of its crown.
- These ecological adaptations of crown architecture, expressed through economic trade-offs among crown traits (Fig 9), have underappreciated impacts upon NIR reflectance and forest functioning.

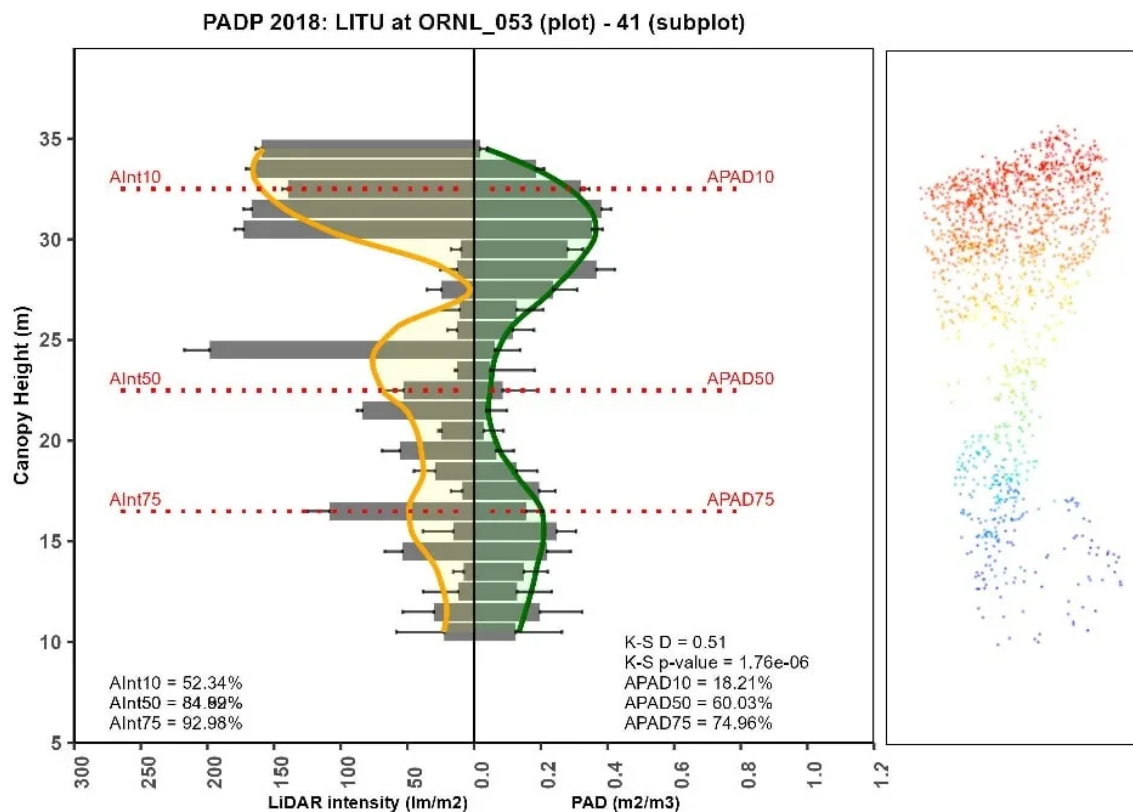
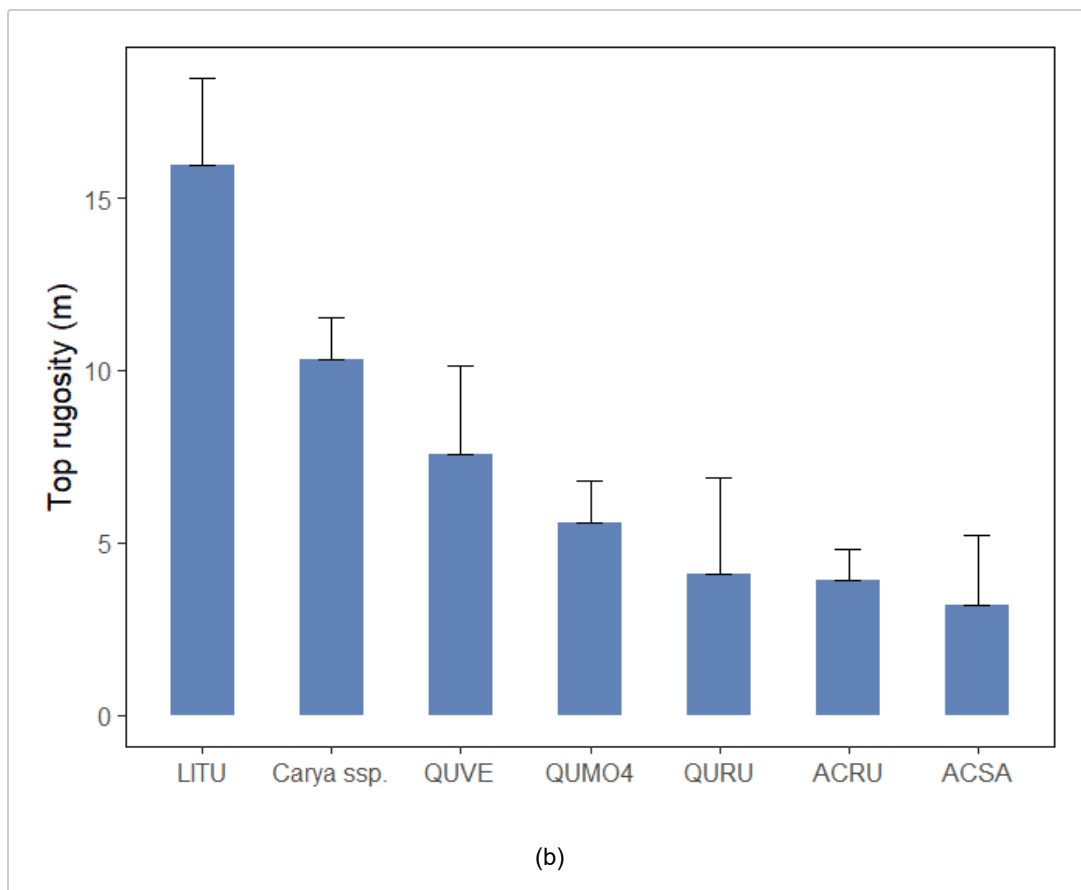
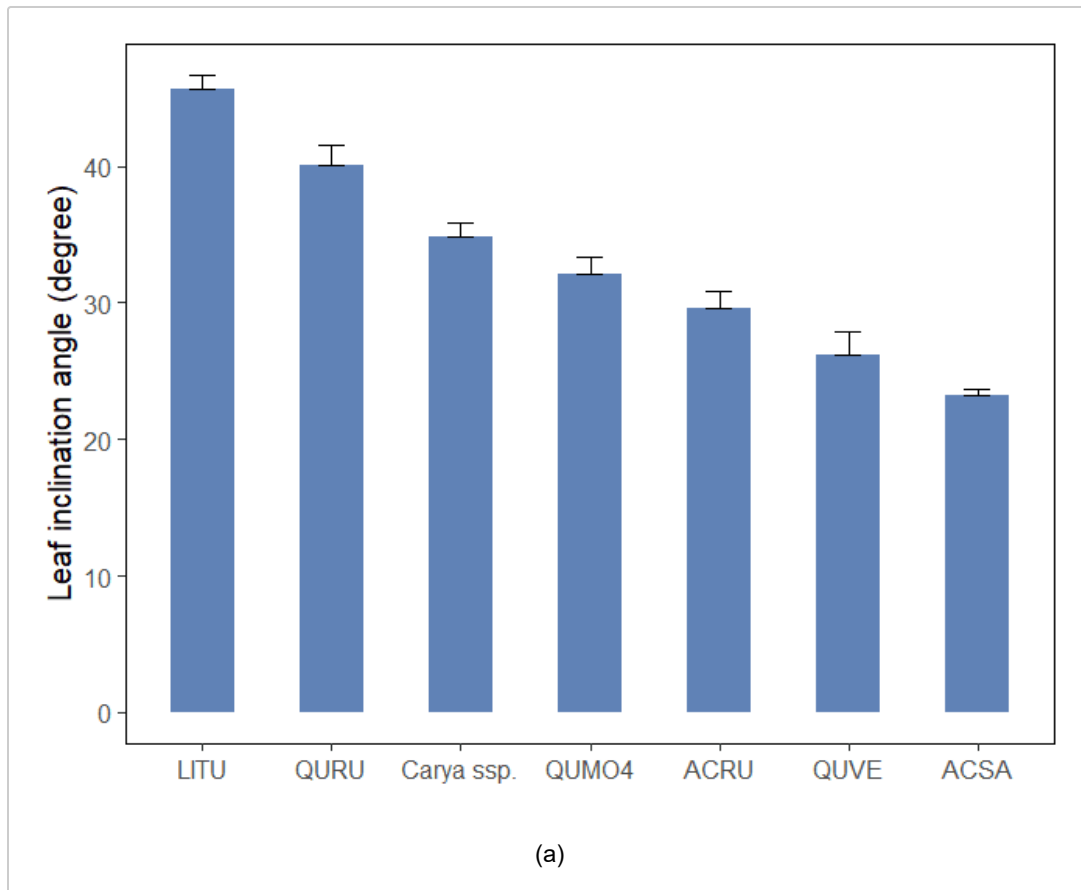


Fig 7: Vertical profiles of the tuliptree at ORNL. Annotations show top 10%/50%/75% APAD (APAD10/50/75) and accumulative intensity (AInt10/50/75)



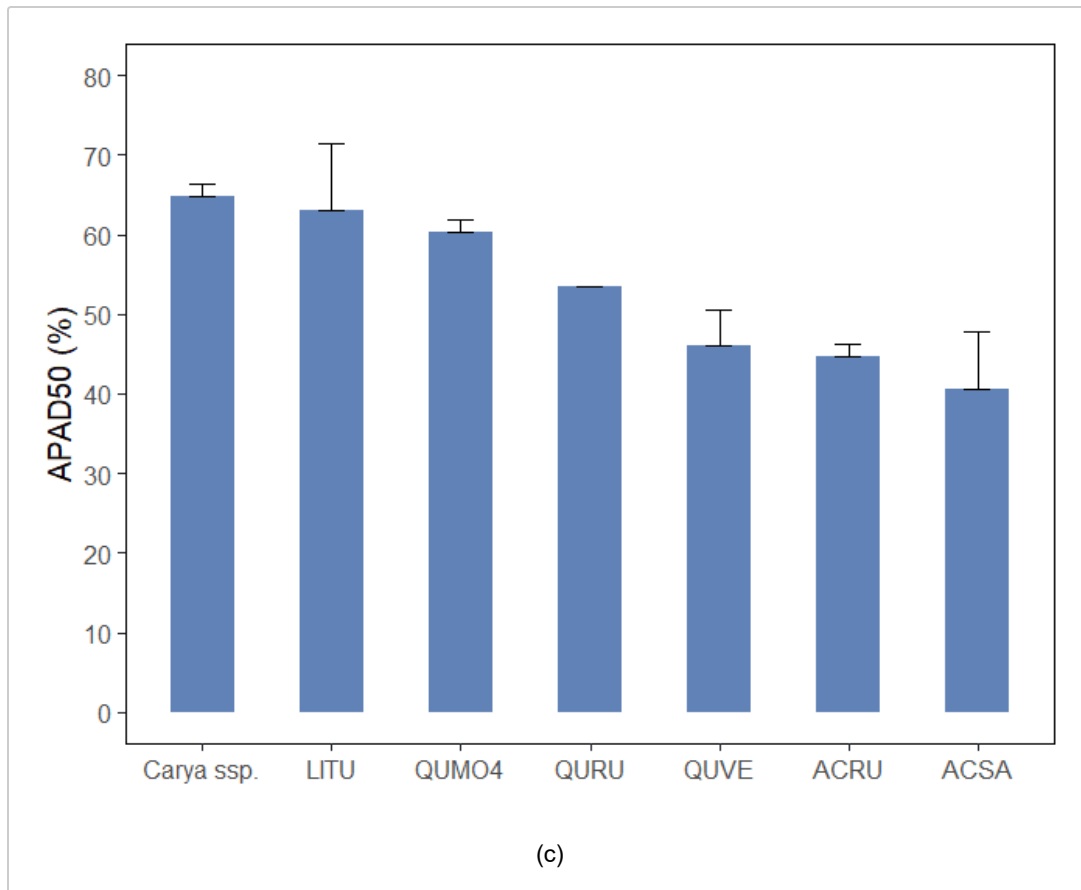


Fig 8: Graphs show (a) MLA, (b) top rugosity (Rt), (c) APAD50 of common species across sites (t-test, $p < 0.05$, error bars show standard errors). Data values are species means

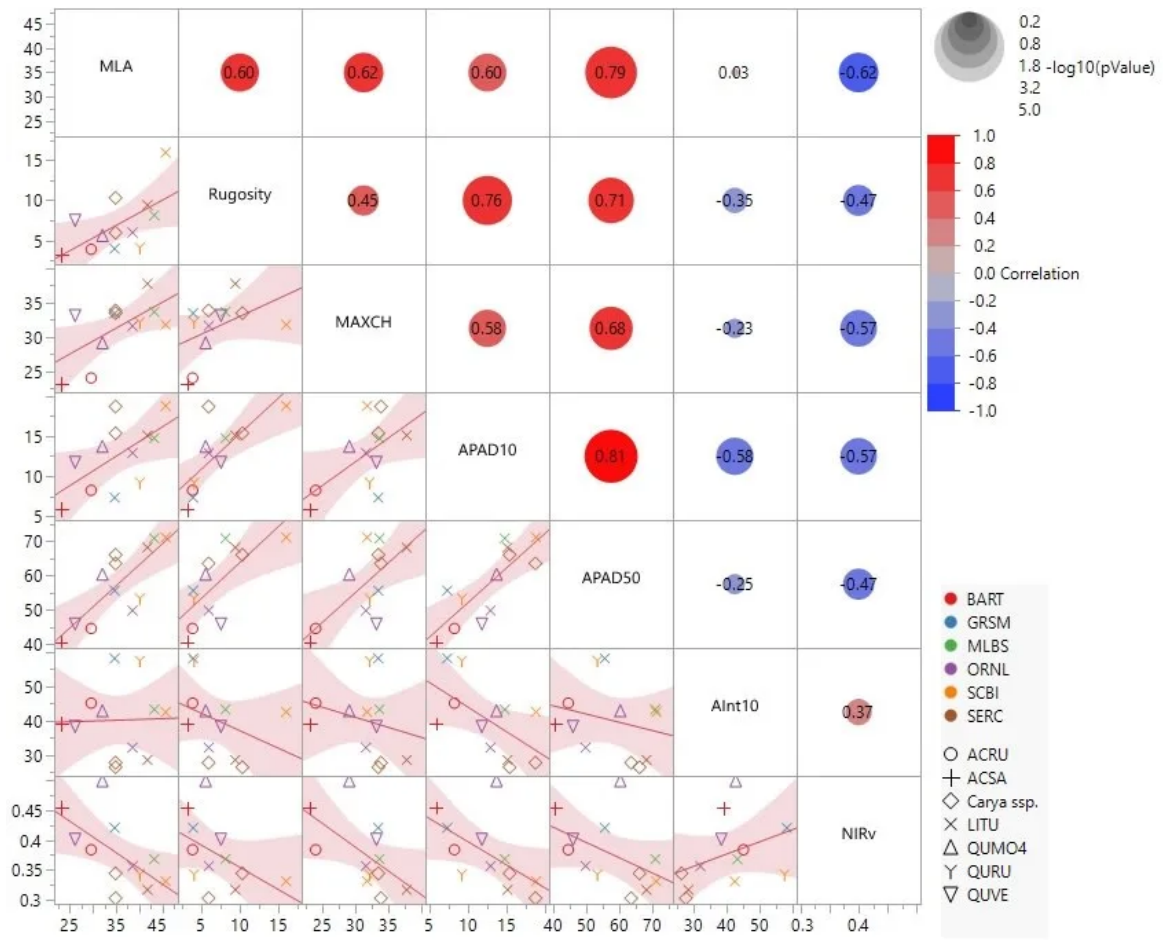


Fig 9: Covariations among 7 traits across all site-species combos. Symbol shape represents species and color represents site. Direction and magnitude of correlations are shown by bubble color (t-test, $p < 0.05$). Data values are species means

5. CONCLUSION & FUTURE WORK

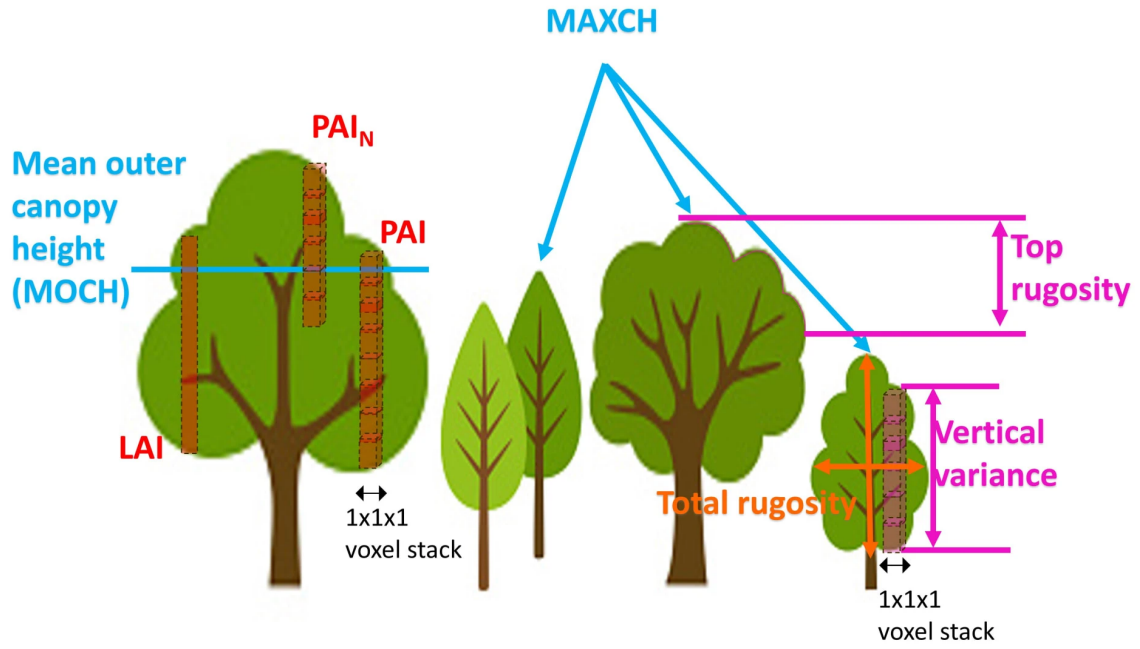
5.1. CONCLUSION

- NEON Data are useful!
- Trees for the Forest. Crown-level process is essential for forest ecology and our object-based analysis is important for Remote Sensing.
- Tree species significantly differ in crown architectural traits as hypothesized.
- Economic tradeoffs exist at crown scale, not just leaves, expressed by the strong co-variations among the crown traits governing how each species adaptively arranges and orients leaves in their crowns as a strategy to harvest sunlight.

5.2. CONCLUSION

- Greatly expand the current hand-delineated sample by delineating artificial-intelligence (AI) tree crowns using deep learning-based model.
- Expand the data at more NEON sites and other biomes representing wider environmental gradients.
- Refine traits to improve delineation of different aspects of crown architecture. For example, the "shape" of the crown may not simply be described by top- or bottom-heaviness due to the multi-modal distribution of many trees. Thus APAD50 alone is not sufficient enough to represent a crown shape.

6. CROWN TRAITS ILLUSTRATION



TRANSCRIPT

ABSTRACT

Tree crown architecture, which we define as the 3-D arrangement and orientation of leaves within a tree crown, influences the rates of photosynthesis, evapotranspiration, and spectral reflectance that affect tree and forest responses to climate change. As part of their adaptive and acclimation strategies for responding to environmental variability, trees are likely to differ in their tree crown architectures, but these differences remain poorly described. We use measurements from 11 deciduous forest locations within the National Ecological Observatory Network (NEON) to quantify traits that can define key dimensions of variability in crown architecture. Specifically, we: (1) measure seasonal trends in mean leaf angle (MLA) from tower-based time-lapse photography, (2) quantify traits describing the density and distribution of leaves in tree crowns from NEON Airborne Observation Platform (AOP) LiDAR data, and (3) infer crown functioning from multi-scale data on near-infrared reflectance of vegetation (NIRv), as obtained from phenocams, the NEON AOP imaging spectrometer, and Harmonized Landsat Sentinel-2 (HLS). From these data, we test for trait covariations (e.g., among MLA, the vertical distribution of plant area index, and the seasonal peak of NIRv) that can suggest fundamental tradeoffs governing how each species arranges and orients leaves in their crowns. In describing how these crown architectural traits covary across the diverse tree species and wide environmental gradients within 11 NEON sites, we highlight implications for tree ecophysiology and remote sensing-based studies on the interactions of trees, forests and climate change.

REFERENCES

- Almeida, D. R. A. D., Stark, S. C., Shao, G., Schiatti, J., Nelson, B. W., Silva, C. A., ... & Brancalion, P. H. S. (2019). Optimizing the remote detection of tropical rainforest structure with airborne lidar: Leaf area profile sensitivity to pulse density and spatial sampling. *Remote Sensing*, 11(1), 92. doi.org/10.3390/rs11010092
- Kamoske, A. G., Dahlin, K. M., Read, Q. D., Record, S., Stark, S. C., Serbin, S. P., & Zarnetske, P. L. (2022). Towards mapping biodiversity from above: Can fusing lidar and hyperspectral remote sensing predict taxonomic, functional, and phylogenetic tree diversity in temperate forests?. *Global Ecology and Biogeography*, 31(7), 1440-1460. doi.org/10.1111/geb.13516
- McNeil et al. (2023) Tree Crown Economics. *Frontiers in Ecology and the Environment* 21:40-48. doi.org/10.1002/fee.2588
- Roussel, J. R., Auty, D., Coops, N. C., Tompalski, P., Goodbody, T. R., Meador, A. S., ... & Achim, A. (2020). lidR: An R package for analysis of Airborne Laser Scanning (ALS) data. *Remote Sensing of Environment*, 251, 112061. doi.org/10.1016/j.rse.2020.112061

